JOURNAL OF AIRCRAFT
Vol. 39, No. 4, July–August 2002

Automated CFD Analysis of Two-Dimensional High-Lift Flows

Anutosh Moitra*
Boeing Commercial Airplane, Seattle, Washington 98124

Validation results are described for an automated process for Navier–Stokes analysis of multielement high-lift configurations in two dimensions. A systematic study of grid requirements for resolving high-lift flowfields is presented, and guidelines are provided for generating grids suitable for resolving flow regimes containing phenomena characterized by widely varying scales, for example, free and confluent wakes and boundary layers, separation and reversed flows. Sensitivities of computed solutions to various grid parameters are documented. The automated software package is validated for slat and flap effectiveness studies, Reynolds-number effects, and gap sensitivities. Results obtained so far show promise of a capability for routine and automated analysis of complex high-lift flows.

Introduction

A CAPABILITY for routine and accurate analysis of aircraft high-lift systems performance is an indispensable requirement for designing aircraft for optimal performance in landing and takeoff phases of flight. Reynolds-averaged Navier–Stokes computational fluid dynamics (CFD) methods have been routinely used for the past decade for analyzing commercial transport airplanes in cruise configuration. However, these methods have not established their ability to predict high-lift system performance consistently or accurately. At present, high-lift system design relies exclusively on wind-tunnel testing to optimize positioning of leading- and trailing-edge devices and overall system performance. Development of accurate predictive tools based on viscous analysis of high-lift flowfields is a pacing item in reducing wind-tunnel testing expenses and expediting the design cycle process.

Flowfields for high-lift systems are characterized by highly complex flow physics, which pose significant challenges to CFD codes. The list of relevant flow physics issues includes laminar flow, attachment line transition, relaminarization, transonic slat flow, confluent boundary layers, wake interactions, separation, and reattachment.[1] A full three-dimensional analysis capability will be ultimately required for comprehensive analysis of these flow features for aircraft in high-lift configurations. However, even for two-dimensional flows state-of-the-art CFD codes are unable to consistently predict increments in performance as a result of changes in Reynolds number and slat/flap positioning.[2] The specialized nature of high-lift aerodynamics necessitates equally specialized CFD methodologies for accurately modeling these phenomena. At present, many of the flow phenomena associated with multielement high-lift airfoils are not well-understood, and the nature and level of adequacy required of CFD processes and tools for accurately representing these phenomena have not been established. Brune and McMasters[3] have noted that formidable problems associated with grid generation, turbulence modeling of separated flows, transition from laminar to turbulent flow, and numerics must be overcome in two dimensions before they can be routinely applied in an airplane design environment. In his landmark paper Smith[4] recognized that techniques verified in two dimensions for resolving fundamental issues, for example, extensions to eddy-viscosity models, do not lose accuracy in three-dimensional applications. Excluding specific three-dimensional phenomena, such as spanwise flow, viscous interference between neighboring airplane components, etc. a two-dimensional CFD study can go far in resolving these theoretical issues and can contribute to laying a basis for consistent analysis of high-lift flows. From a practical point of view, a two-dimensional viscous analysis capability will be very useful for predicting high-lift system performance trends with respect to variations in Reynolds number and geometric parameters such as flap and slat settings. Substantial need exists in the aircraft industry for developing an automated CFD software system capable of routinely and accurately analyzing two-dimensional high-lift configurations with minimum user interaction. The goal of the present project is to automate all phases of the analysis process comprising 1) geometry preprocessing including positioning of elements, 2) grid generation, 3) flow solving, and 4) postprocessing of results. The software system uses the unstructured grid-generation code AFLR2[5] and the unstructured grid flow solver NSU2D.[6] The proposed paper will report on validation of this software tool with respect to its ability to predict performance trends of high-lift systems.

Available literature on validation of two-dimensional high-lift analysis tools against wind-tunnel test data indicates that CFD tools have so far been unreliable as predictive tools. An extensive review of results obtained as part of a CFD Challenge Workshop held in 1993 has been given by Ying.[7] Results from this workshop demonstrate wide disparities between predictions from various codes. Consistency in matching test data has not been achieved even with the opportunity to tune the grid or the flow solver to specific configurations. Given these difficulties in validating isolated cases, it is easy to appreciate the challenges presented by the need to predict performance trends for varying Reynolds numbers and geometric configurations. Validations of performance trends are, therefore, rarely attempted. These challenges are further compounded in the context of automation by the absence of the luxury of modifying the grid and the flow solver according to the needs of individual cases. To meet this challenge successfully, the developer must identify the sensitivities of the solution to grid parameters and the flow solver. Strategies for adequately handling these sensitivities for the expected range of configurations must be built into the software system. The resulting software must then be validated for a wide range of configurations to ensure accurate prediction of trend data.

Solution Sensitivities

Sensitivities of the computed solution belong to two categories: those dependent on the grid and those influenced by attributes of the flow solver. Some issues in grid sensitivities of the solution have been addressed previously by the author in Moitra.[8] Grid attributes such as surface point distribution, normal spacing near the surface, grid stretching ratio, and grid density in wake regions have large effects on the accuracy of the computed solution for complex high-lift flows. Although some guidelines exist in literature regarding

Received 12 November 2001; revision received 8 April 2002; accepted for publication 15 April 2002.

*Principal Engineer, P.O. Box 3707 MC 67-LF; anutosh.moitra@boeing.com. Associate Fellow AIAA.

acceptable grid parameters for boundary-layer flows, a reliable set of grid attributes necessary and sufficient for resolution of complex and interacting wake flows is currently unavailable. A self-consistent method has been developed for providing specific control over grid density in boundary layers as well as wakes through optimal control of the spacing at the surface of the wing and the stretching ratio. The method provides a reliable means for studying grid convergence of computed solutions. Subsequent sections of the paper will describe optimal grid parameters established through validation studies and illustrate their efficacy in capturing correct performance trends. Recommended parameter values are listed in the grid convergence summary section.

Among attributes of the flow solver, turbulence models and transition location are the principal sources of solution sensitivity. Subtle differences in turbulence models can cause significant differences in the prediction of wake growth particularly for wakes in adverse pressure gradients, which characterize high-lift flowfields. This can lead to inaccurate predictions of wake spreading and consequently inaccuracies in predictions of maximum lift. Proper specification of transition location is crucial to accurate predictions of Reynolds-number trends. The extent and location of separation are strongly influenced by the location of transition from laminar to turbulent flow. In computational studies a fully turbulent flow is generally assumed in cases where transition is close enough to the leading edge to justify use of this assumption. A detailed study of turbulence models and transition methods is beyond the scope of this paper. The present study was conducted assuming fully turbulent flow modeled by the Spalart–Allmaras turbulence model[9] except where noted otherwise.

Grid Sensitivities

A consistent method for studying convergence of the computed solution with increasing grid density is an important prerequisite for validating an automated CFD analysis procedure. Consistency of the grid system is difficult to achieve in analyzing high-lift flows. The difficulty arises out of the need to ensure sufficient grid density in regions of interesting flow phenomena while preventing deterioration of grid density and smoothness in other areas. The problem is further compounded by a lack of guidelines regarding grid resolution requirements for the complex flow physics involving disparate length scales that arise in flowfields of multielement high-lift configurations. The three principal areas of interest in the grid system are resolution of the boundary layer, grid density on the surface of the geometry, and resolution of wakes including regions of merging or separation. A parametric study was performed to establish grid attributes necessary for ensuring adequate grid resolution for automated computation of high-lift flows. A three-element airfoil, previously studied by Lynch et al.,[2] was used as the test configuration in this study of grid sensitivity. The airfoil geometry[2] is shown in Fig. 1. Grid parameters were varied to increase grid density until no discernible changes in the computed results were noticeable. Surface distributions of pressure and skin-friction coefficients as well as integrated performance quantities, for example, lift and drag coefficients, were monitored in order to establish grid convergence of the solution. Results of the study are described next.

Surface Grid Density

Distribution of points on the surface of the geometry is controlled by clustering grid points in regions of high curvature and limiting the maximum allowable spacing between any two adjacent points to a specified value. The latter is necessary in order to ensure adequate grid resolution in areas of low curvature, for example, the region near the trailing edge. This limiting value of the spacing between adjacent surface points was decremented until a grid-converged solution was obtained. No changes in the computed solution were noticeable when this parameter was decremented below a value of 0.3% of the chord, thus establishing this as the optimal surface grid parameter value. Details of a grid convergence study performed in order to establish this value are presented in the grid convergence summary section. Grid densities in the leading- and trailing-edge regions require special attention. In a previous study done at Boeing, the maximum limits on surface spacing were established to be 0.1 and 0.3% of the chord at leading and trailing edges, respectively. A curvature-weighted Poisson method was used to generate the surface grid in the present study. Because of curvature-based clustering, the spacing at the leading edge never exceeded 0.05% of the chord. The upper limit of 0.3% chord on spacing anywhere on the airfoil automatically satisfies the trailing-edge spacing requirement. Additional clustering near the trailing edge reduced the trailing-edge spacing further below this prescribed limit.

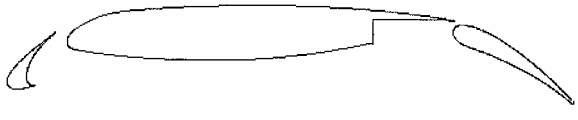

Fig. 1 Three-element high-lift configuration.

Boundary-Layer Resolution

Grid resolution requirements for boundary layers are well-established in available literature and have been reviewed by the author in Moitra.[8] Initial normal spacing and stretching ratio are the two principal parameters in this context. Initial normal spacing at the surface must be small enough to provide at least three points in the linear sublayer defined as the region bounded by $y^+ < 5$. This was ensured in the procedure implemented in this study. A plot of surface variation of y^+ in the computed solution for all three elements of the test airfoil, presented in Fig. 2, shows an upper bound of approximately 1.5 on surface y^+.

An upper limit on the value of the stretching ratio has been established by Spalart[10] based on an analysis of optimal grid distributions with regard to truncation errors. According to this analysis, optimal grid distribution is obtained for a geometric stretching ratio not exceeding 1.2. Smaller values of the stretching ratio produce higher resolution at the cost of rapid increases in the number of grid points.

Wake Resolution

Resolution of wake regions is perhaps the most crucial requirement for accuracy of CFD predictions of high-lift flows. Guidelines for grid resolution of wakes, however, are scarce in available literature. In the absence of appropriate adaptive grid generation methods capable of modeling wakes, the usual method employed for wake resolution consists of a priori specification of wake locations in the form of lines in the flowfield and clustering grid points in their vicinity in the same manner as for boundary layers. The geometry of the predefined wake line is determined either from the geometry of the airfoils or from wake shapes predicted by flowfield solutions obtained by potential flow codes. A major difficulty with this procedure is that wake positions predicted by Navier–Stokes methods rarely coincide with these prescribed wake locations. This is not surprising because potential flow wakes are not likely to be true representations of wakes for high angles of attack or large flap deflections. Therefore, this method of attempting wake resolution results in a waste of grid points at best and corruption of the solution as a result of lack of resolution where needed at worst.

A systematic analysis of grid requirements for wakes is necessary for resolving the issues just stated. Wakes start as boundary layers. This causes no difficulty because wakes, at their points of genesis, are submerged within the boundary-layer grid and are well resolved. As the wake from the leading-edge element moves downstream over the following element, it emerges from the boundary-layer grid as it moves away from the airfoil surface. A lack of grid resolution will cause rapid dissipation of the wake in this case. To determine what degree of grid density will provide adequate resolution, we must consider the rate of spreading of the spatial width of wakes. An examination of velocity profiles in a typical wake and a boundary layer reveals that velocity gradients in the boundary layer are hundreds and often thousands of times larger than wake velocity gradients. Furthermore, the wake half-width grows in direct proportion to $x^{1/2}$, where x is streamwise distance. A typical airfoil length is several

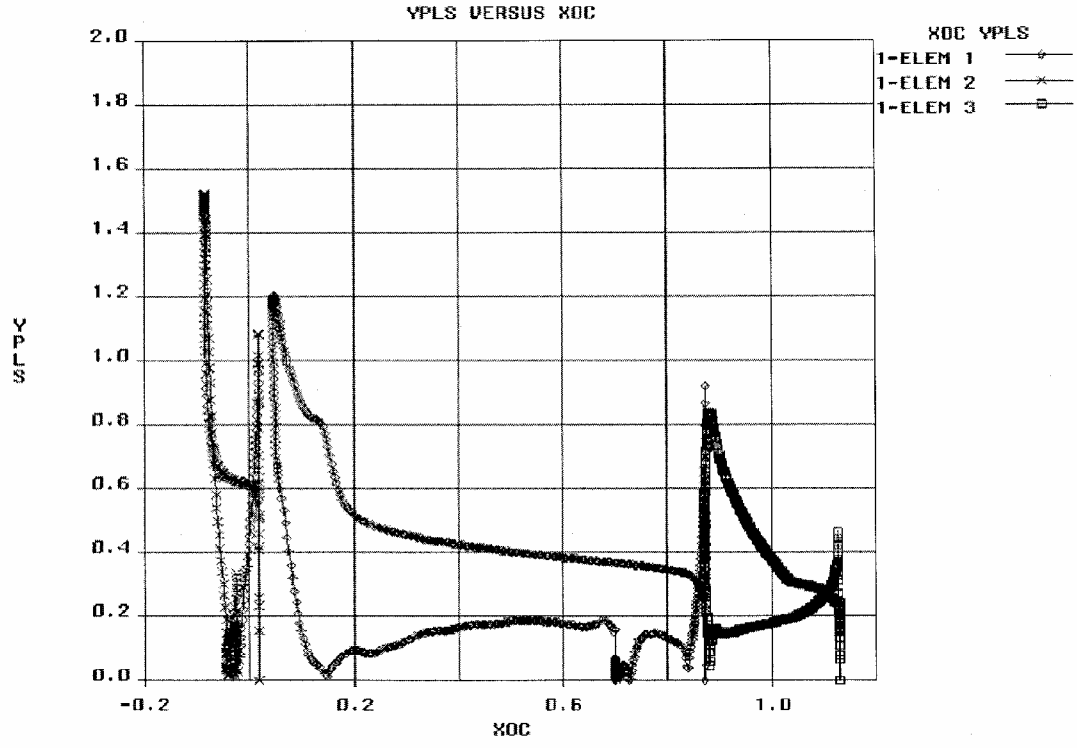

Fig. 2 Variation of Y^+ along surface.

orders of magnitude larger than the typical boundary-layer thickness. Therefore, it becomes clear that the width of the wake grows several orders of magnitude larger than the boundary-layer thickness as the wake traverses the length of the airfoil. The preceding rationale indicates that it is reasonable to expect that a grid spacing several orders of magnitude larger than that required for boundary layers should be sufficient for resolving wakes. Grid density in the wake region can be controlled using the stretching ratio as a convenient parameter. Lowering the value of the stretching ratio increases grid density in the wake region and produces a dense band of grid covering the boundary layer as well as the wake region.

The region downstream of the main element and covering the flap wake warrants special attention. For highly deflected flaps the flowfield in this region is characterized by flow separation, often massive, or off-body flow reversal. These phenomena occupy a large spatial extent and cannot be adequately resolved by grid refinement of the near-body region alone. A novel concept is utilized in this study for resolution of this region. A box is defined extending from the leading edge of the flap to some distance downstream of the trailing edge of the flap. The box is filled with densely packed grid points with a uniform distribution. This technique is based on the rationale given previously by the author[8] that the widely varying scales associated with flow phenomena arising in this region, for example, wakes, boundary layers, reverse flow regions, etc., will cause even a solution-adapted grid to approach a uniform grid. This rationale appears to be verified in adaptive grid results presented by Walsh and Zingg[11] in their paper describing solution adaptation of unstructured grids. The cell size in this box matches that at the edge of the boundary layer of the flap. The boundary-layer grid is not disturbed. This procedure for generating the grid system provides an integral methodology for ensuring grid resolution of boundary layers as well as wake regions. The principal parameters for grid control are the stretching ratio and the limiting value of surface spacing. This methodology allows consistent grid convergence studies for establishing the necessary and sufficient values of these parameters. In this study the value of the stretching ratio was systematically varied to establish a lower limit below which no changes in the computed solution were noted. This lower limit on the stretching ratio was determined to be 1.1. Using values lower than 1.1 causes very rapid increase in the number of grid points with no accompanying change in the solution. The corresponding value of cell size in the uniformly spaced box was approximately 0.25% of the chord. A representative grid system generated using the methodology just described is shown in Fig. 3.

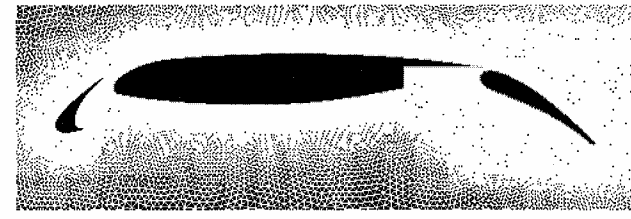

Fig. 3 Grid system for high-lift configuration.

Grid Convergence Summary

Necessary and sufficient attributes of grid systems for computing high-lift flowfields were established by systematically varying grid parameters until an increase in grid density no longer produced appreciable variations in surface pressure and skin-friction coefficients as well as integrated quantities such as coefficients of lift, drag, and moment. The grid convergence study was performed using the airfoil geometry,[2] shown in Fig. 1. The flow conditions used for this study were $M = 0.2, \alpha = 19$ deg, and $Re = 9 \times 10^6$. Flowfields were computed for seven different grids. The grid parameters and corresponding computed force and moment coefficients are presented in Table 1.

Convergence of velocity profiles in the wake with respect to grid density is illustrated in Fig. 4. An experimentally obtained velocity profile at the midchord station on the flap is plotted together with computed results from grids A, C, and D. This represents a 150% increase in grid size from the coarsest to the finest of these three grids. It can be seen that the computed velocity profile converges with increasing grid density and compares reasonably well with the experimental profile. The difference between the results obtained with grids A and C are small enough to establish a value of 1.1

Table 1 Grid parameters used in grid convergence study

Case name	Ds_{max}[a]	Stretching ratio	Number of grid points	C_L	C_D	C_M
A	0.005	1.1	215,240	4.26105	0.06022	−0.8387
B	0.005	1.15	146,319	4.26686	0.06075	−0.8389
C	0.005	1.2	119,130	4.28775	0.05902	−0.8459
D	0.005	1.3	86,242	4.32101	0.05879	−0.8517
E	0.003	1.1	250,348	4.26573	0.05986	−0.8386
F	0.008	1.1	206,165	4.23126	0.06207	−0.8313
G	0.01	1.1	189,012	4.18204	0.06487	−0.8186

[a] Ds_{max} = maximum allowed spacing between surface points.

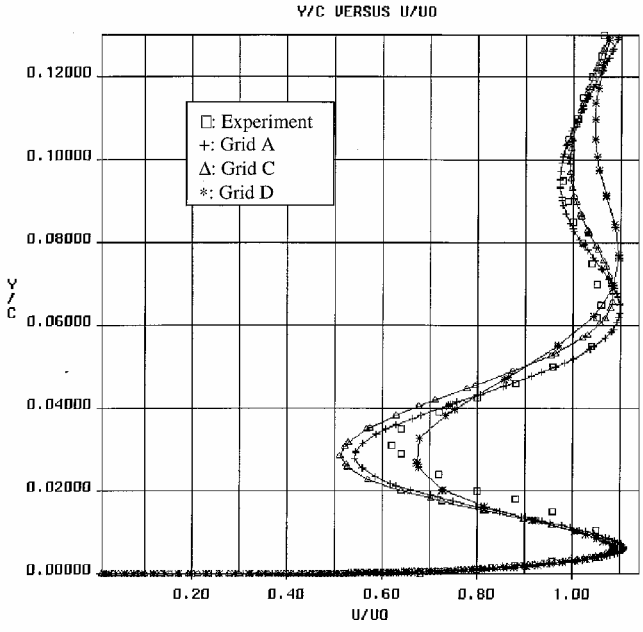

Fig. 4 Grid convergence of wake velocity profile.

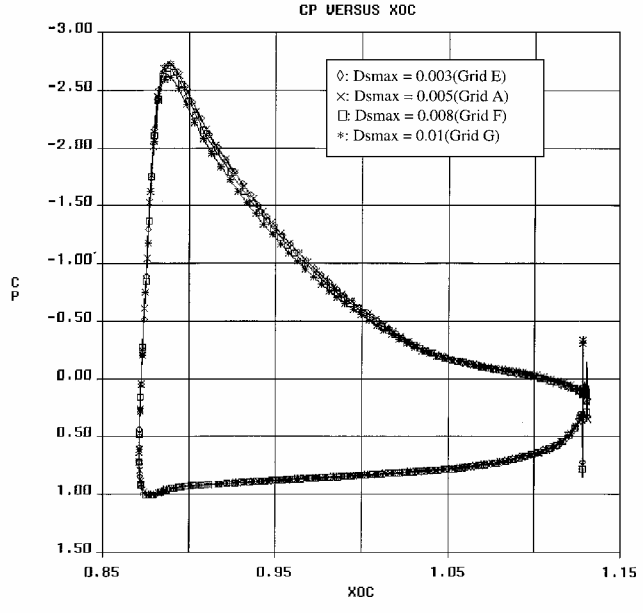

Fig. 5a Effect of Ds_{max} on C_P profile.

for the stretching ratio as sufficiently small to ensure accuracy of prediction.

Convergence of surface pressure and skin-friction coefficients with increasing grid density was investigated next. Effects of reducing ds_{max}, the maximum allowed spacing between adjacent points on the surface, on surface distribution of pressure coefficient are illustrated in Figs. 5a and 5b. Results computed with grids E, A, F, and G are plotted in Fig. 5a. These grids represent a total increase

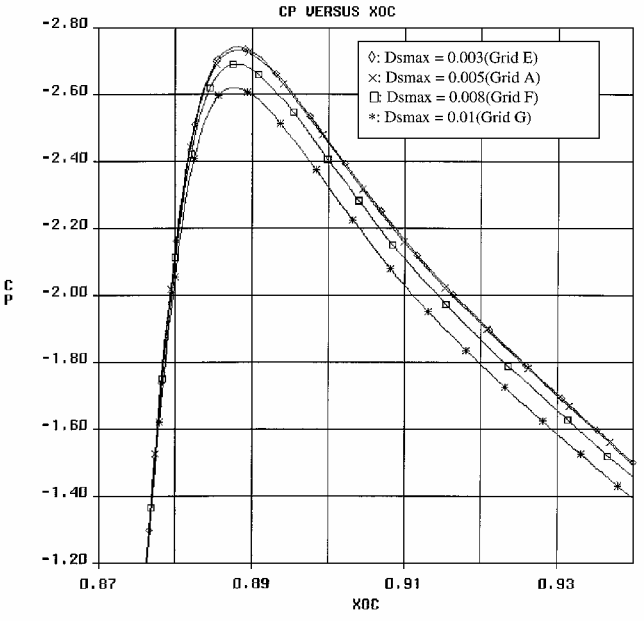

Fig. 5b Effect of Ds_{max} on C_P profile (leading-edge region).

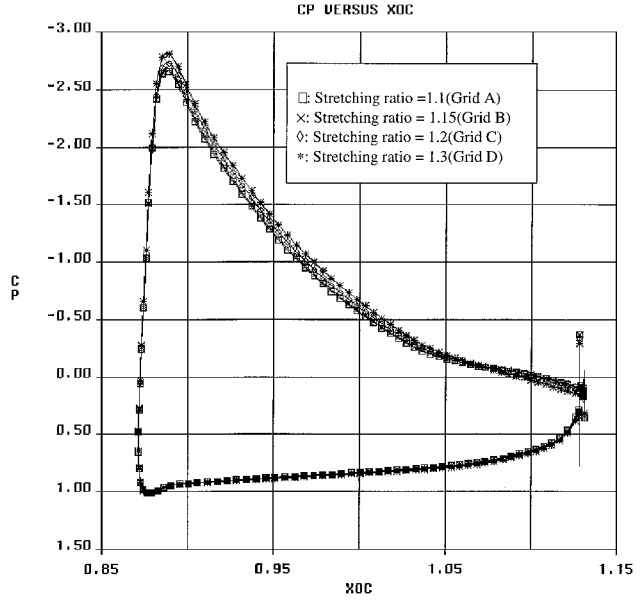

Fig. 6a Effect of stretching ratio on C_P profile.

in the value of ds_{max} from 0.3 to 1.0% of the chord. An enlarged view of the leading-edge region is shown in Fig. 5b. The pressure coefficient is seen to have converged sufficiently for a value of ds_{max} equal to 0.3% of the chord. The difference between the results of grids E and A is very small, and nothing is to be gained from further reduction of the value of ds_{max}.

Convergence of pressure coefficient profiles with decreasing values of the stretching ratio is presented in Figs. 6a and 6b. Computed profiles for grids A, B, C, and D are plotted together for comparison in Fig. 6a. The enlarged view of the leading-edge region presented in Fig. 6b indicates convergence of the computed results at a value of 1.1 for the stretching ratio.

Variation of the computed skin-friction coefficient is investigated next. An enlarged view of skin-friction profiles in the leading-edge region computed using grids E, A, F, and G is shown in Fig. 7. Convergence is indicated for a value of ds_{max} equal to 0.3% of the chord. Effect of stretching ratio on computed skin-friction profiles is illustrated in Fig. 8. Results computed with grids A, B, C, and D are plotted together for comparison. Convergence is clearly indicated at a value of 1.1 for the stretching ratio.

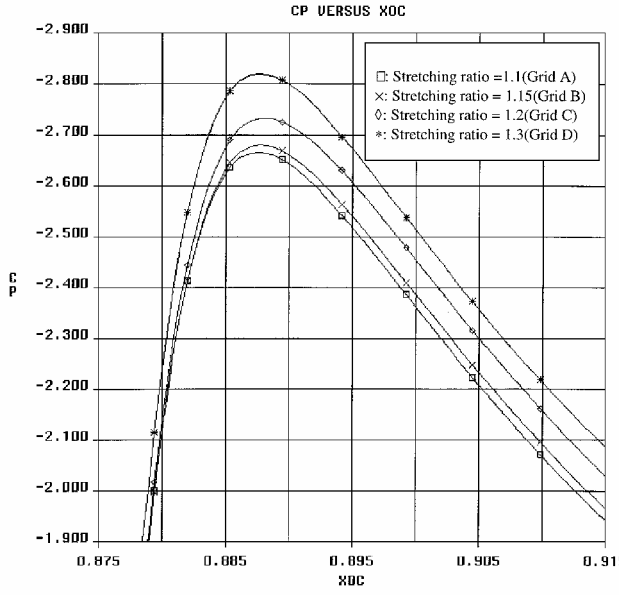

Fig. 6b Effect of stretching ratio on C_P profile (leading-edge region).

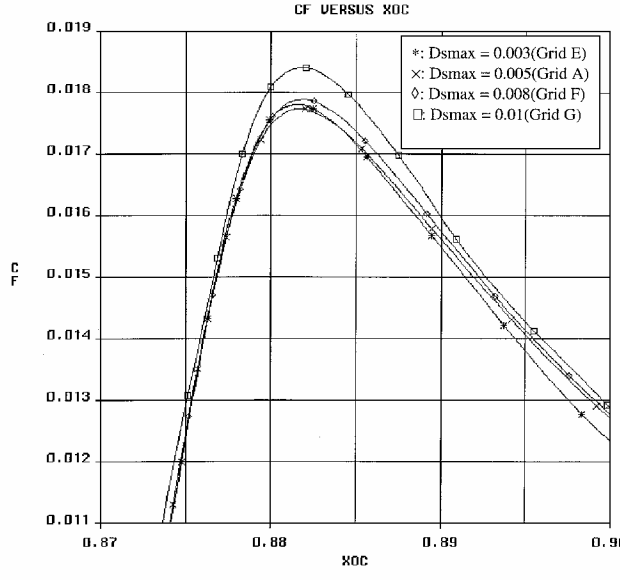

Fig. 7 Effect of Ds_{max} on C_F profile.

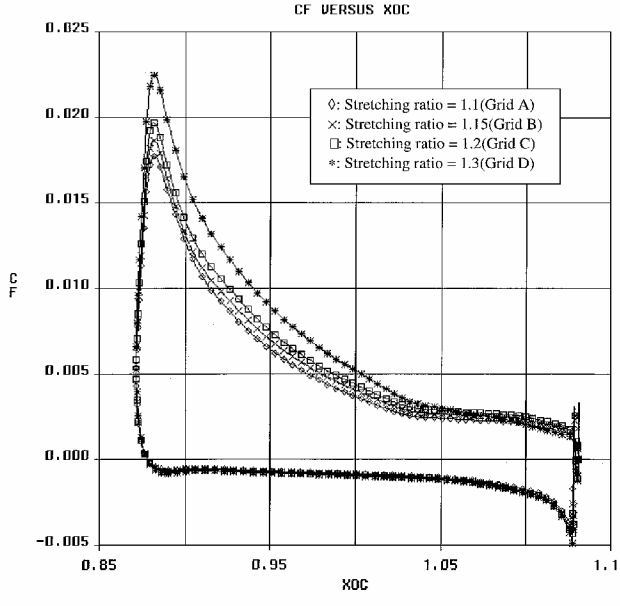

Fig. 8 Effect of stretching ratio on C_F profile.

Table 2 Recommended grid control parameter values

Grid control parameter	Recommended value
Stretching ratio	1.1
ds_{max}	0.003*chord

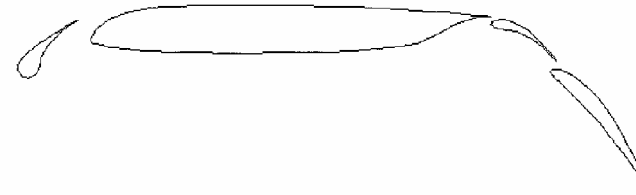

Fig. 9 Geometry of double-slotted four-element airfoil.

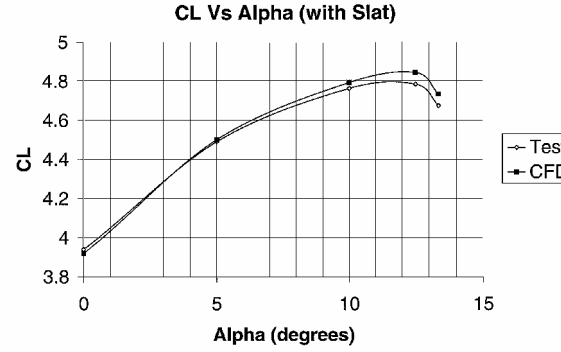

Fig. 10 Variation of lift coefficient with angle of attack for four-element airfoil with gapped slat.

The necessary and sufficient values of grid control parameters established in this study are listed in Table 2.

CFD Challenges and Validation

Johnson[12] has given a concise review of the challenges facing developers of CFD methods for predicting performance trends of high-lift systems. These challenges have been categorized in four classes: slat effects, flap effectiveness, gap sensitivities, and Reynolds-number effects. The goal of the present undertaking at Boeing is to address each of these challenges within the framework of an automated high-lift analysis tool. Validation of this emerging capability is an essential prerequisite for adoption of the tool by industry with confidence. Representative results obtained for validation of each of these challenge areas are presented next.

Slat Effects

A CFD tool must possess the ability to predict increments in drag and maximum lift caused by a gapped slat in order to be useful to the high-lift design engineer. A four-element airfoil with a gapped leading-edge slat and a double-slotted trailing-edge flap assembly[13] was investigated for variation of the lift coefficient with the angle of attack. The airfoil geometry is shown in Fig. 9. The deflections for the leading-edge element, the forward flap, and the aft flap were 45, 30, and 50 deg, respectively. Computed CFD results are plotted in Fig. 10 against angle of attack together with test data[13] obtained for a Mach number of 0.2 and a Reynolds number of 2.83×10^6. A good match is noted between test data and CFD results. The main effect of an extended flap is to delay the angle of stall.[4] Correct modeling of the slat is therefore crucial to correct prediction of stall angle. The predicted maximum value of the coefficient of lift is seen in Fig. 10 to occur at the correct angle of attack indicating proper modeling of slat performance.

Flap Effectiveness

The ability to accurately predict lift increments as a result of changes in flap deflections is essential to the high-lift designer.

Fig. 11 Geometry of single-slotted airfoil.

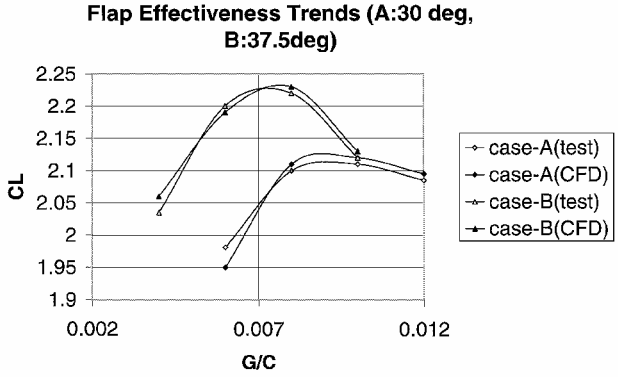

Fig. 12 Variation of lift coefficient with flap angle.

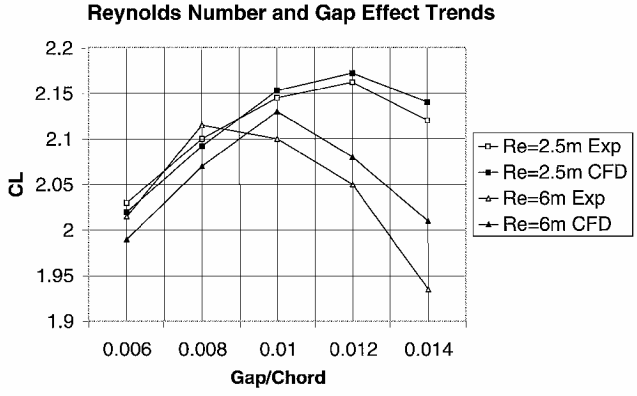

Fig. 13 Variation of lift coefficient with Reynolds number and gap size.

Configuration decisions (for example, double- or single-slotted flaps) rely on accurate assessment of flap effectiveness. The ability of the Boeing CFD tool to predict flap effectiveness was tested using a single-slotted airfoil geometry[14] shown in Fig. 11. Transition locations for this case were available from test data[14] and were used in the computation. Computed lift coefficients have been plotted in Fig. 12 against varying gap size for this single-slotted flap system for two flap settings. Results for flap deflections of 30 and 37.5 deg are presented for a Mach number of 0.18, a Reynolds number of 23.0×10^6, and an angle of attack of 2.0 deg. Computed results are compared with test data.[14] Values predicted by CFD show sufficient accuracy for engineering application.

Reynolds-Number Effects

Optimal aircraft design hinges on the ability to predict airplane performance in flight. A CFD method capable of providing accurate estimates of variation of high-lift system performance with increasing Reynolds number is indispensable for this purpose. Computed trends in Reynolds-number scale effects in high-lift flows are presented in Fig. 13. Transition locations for this case were available from test data[14] and were used in the computation. Computed and experimental[14] values of lift coefficient are plotted for a single-slotted airfoil for two Reynolds numbers (2.5 and 6.0×10^6) for a range of gap sizes. The flap deflection was 30 deg, and the Mach number and angle of attack were 0.18 and 2.0 deg, respectively. Good agreement between test data and CFD predictions is noted. Results computed at a higher Reynolds number of 23×10^6 shown in Fig. 12 showed similar agreement.

Gap Sensitivities

At present, optimization of leading- and trailing-edge devices relies on expensive and time-consuming wind-tunnel testing. Performance of a slotted airfoil is heavily dependent on the nature of flow through the slots. Flowfields inside and in the vicinity of slots are extremely complex and difficult to model accurately. Effects of gap size on lift increment are not monotonic. Maximum lift increment is achieved for an optimal value of the gap size. Accurate prediction of this optimal gap size is of crucial importance to high-lift system designers. A reliable CFD capability to predict increments in lift and drag as a result of changes in flap gap and overlap will significantly reduce the cost and cycle time of high-lift system design. The ability of the present CFD tool in predicting gap sensitivities has been demonstrated in Figs. 12 and 13 for a range of flow conditions and geometric configurations. Very good agreement with test data is noted in all cases.

Conclusions

The automated CFD tool for high-lift system analysis currently under development at Boeing has shown promise of being an accurate tool for routine use. Validation data for performance trends as well as validation of flow physics characterizing high-lift flowfields have established the efficacy of the proposed grid-generation techniques in generating accurate flow solutions. The gridding methodology provides a consistent framework for studying grid convergence of the computed solution and will be useful in future studies of turbulence models and transition locations.

References

[1]Meredith, P. T., "Viscous Phenomena Affecting High-Lift Systems and Suggestions for Future CFD Development," *High-Lift System Aerodynamics*, AGARD-CP-15, Paper 19, 1993, pp. 19.1–19.8.

[2]Lynch, F. T., Potter, R. C., and Spaid, F. W., "Requirements for Effective High Lift CFD," *International Council of the Aeronautical Sciences Proceedings*, Vol. 2, 20th Congress, AIAA, Reston, VA, Sept. 1996.

[3]Brune, G. W., and McMasters, J. H., "Computational Aerodynamics Applied to High-Lift Systems," *Applied Computational Aerodynamics*, edited by P. A. Henne, Progress in Aeronautics and Astronautics, Vol. 125, 1990, pp. 389–413.

[4]Smith, A. M. O., "High-Lift Aerodynamics," *Journal of Aircraft*, Vol. 12, No. 6, 1975, pp. 501–530.

[5]Marcum, D. L., "Generation of Unstructured Grids for Viscous Flow Applications," AIAA Paper 95-0212, Jan. 1995.

[6]Mavriplis, D. J., "Turbulent Flow Calculations Using Unstructured and Adaptive Meshes," *International Journal for Numerical Methods in Fluids*, Vol. 13, No. 9, 1991, pp. 1131–1152.

[7]Ying, S. X., "High Lift: Challenges and Directions for CFD," *AIAA/NPU AFM Conference Proceedings*, China, June 1996.

[8]Moitra, A., "Unstructured Grid Issues in 2-D High-Lift Computations," *Proceedings of the 7th International Conference on Grid Generation in Computational Field Simulations*, International Society of Grid Generation, Whistler, BC, Canada, Sept. 2000, pp. 263–274.

[9]Spalart, P. R., and Allmaras, S. R., "A One-Equation Turbulence Model for Aerodynamic Flows," AIAA Paper 92-0439, Jan. 1992.

[10]Spalart, P. R., "Trends in Turbulence Treatments," AIAA Paper 2000-2306, June 2000.

[11]Walsh, P. C., and Zingg, D. W., "Solution Adaptation of Unstructured Grids for Two-Dimensional Aerodynamic Computations," *AIAA Journal*, Vol. 39, No. 5, 2001, pp. 831–837.

[12]Johnson, P. L., Jones, K. M., and Madson, M. D., "Experimental Investigation of a Simplified 3D High Lift Configuration in Support of CFD Validation," AIAA Paper 2000-4217, Aug. 2000.

[13]Omar, E., Zierten, T., Hahn, M., Szpiro, E., and Mahal, A., "Two-Dimensional Wind-Tunnel Tests of a NASA Supercritical Airfoil with Various High-Lift Systems," NASA CR-2215, Sept. 1973.

[14]Payne, F. M., "LTPT-5 Two-Dimensional Wind Tunnel Test of a Single Slotted Flap and Comparison with a 2D Navier–Stokes Code," Document D6-81693, Boeing, Seattle, WA, 1995.